A comparative study of tungsten erosion-redeposition in divertor sheaths versus RF sheaths on WEST

A. Renganathan[(a)], D. Curreli[(a)]
(a) University of Illinois at Urbana Champaign, Illinois, USA
Session UP11, Poster Session VIII, Poster UP11.00052
65th Annual Meeting of the APS Division of Plasma Physics, Denver, CO, October 31, 2023

Overview

- We conducted a comparative computational analysis of the two regions that are expected to contribute to most tungsten (W) impurity production on the WEST tokamak, namely (1) the divertor and the (2) RF limiters
- Our analysis focused on the fundamental understanding of the near-surface behavior of the W impurities as they enter the plasma sheaths
- The analysis was carried out in two steps:
  (1) Analysis of tungsten emission from the surface and subsequent ionization in the plasma; determination of the first-ionization distribution;
  (2) Local impurity transport and their interaction with the sheaths, aimed at an accurate determination of prompt (local) redeposition.
- In particular, the study focused on determining the prompt-redeposition fraction of impurities in the expanding/contracting field of RF sheath, and compare that against the case of the quiescent thermal sheath encountered at the divertor.

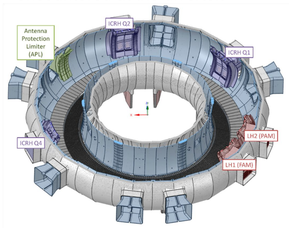

Figure 1. WEST Top and 3D cut view. ICRH antennas are named after the equatorial port (Q) number they are inserted in: Q1, Q2 and Q4. The lower divertor and the buffle are visible at the bottom of the image (Figure credits [4])

Relevant WEST Conditions

Conditions along the surface of the RF Limiter

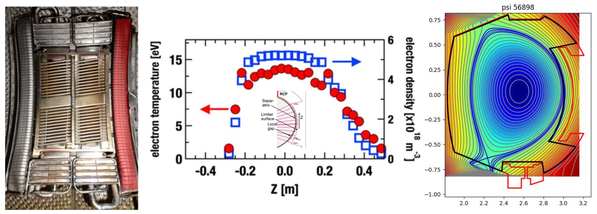

(a) (b) (c)

Figure 2. (a) Image of the WEST ICRH antenna Q2 with IC2R limiter highlighted in red (photo source [2]); (b) electron density (blue) and electron temperature (red) measured spectroscopically from OES along the vertical extension of the RF limiter (figure source [2]); (c) magnetic flux surfaces for WEST shot #56898.

Conditions at the lower divertor

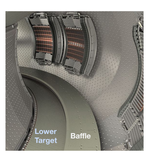

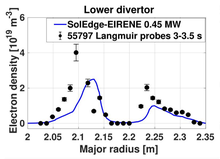

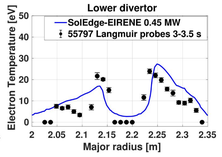

(a) (b) (c)

Figure 3. (a) CAD rendering of the inner vessel of WEST, showing the location of lower diverter and baffle (source: Hillaret); (b) electron density, and (c) electron temperature along the lower divertor as measured using Langmuir probes (black dots) and calculated using SolEdge-EIRENE, for WEST Show #55797. The two peaks correspond to the inner and outer targets.

Divertor Sheath

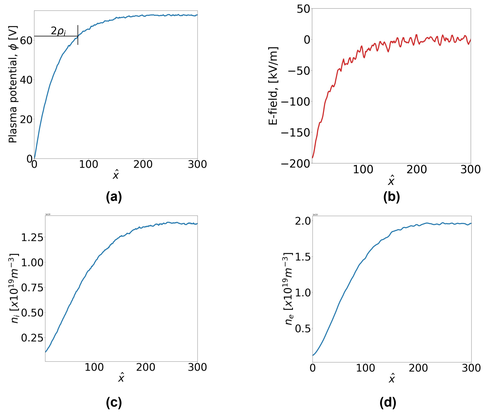

(a) (b) (c) (d)

Figure 4. Structure of steady state thermal sheaths for the divertor conditions in WEST: He plasma made of 90% He^{2+} and 10% He^{+} with n_e=2x10^{19}m^{-3}, T_i=T_e=25eV, B=3.7T, magnetic angle ψ=88.59°. Profiles: (a) plasma potential, (b) electric field, (c) ion density, (d) electron density as functions of spatial domain.

RF Sheath

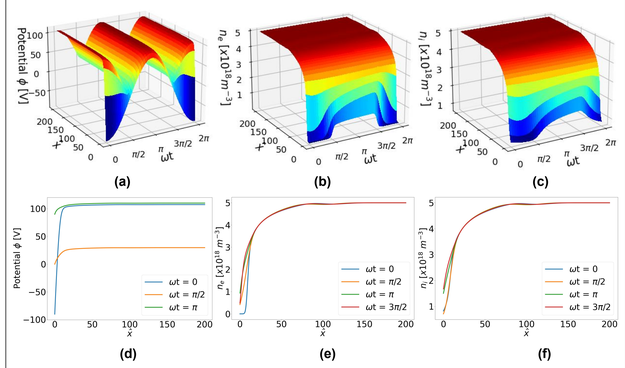

(a) (b) (c) (d) (e) (f)

Figure 7. RF sheath model for RF limiter conditions in WEST: Singly ionized He plasma with n_e=5x10^{18}m^{-3}, T_i=T_e=12eV, B=3.7T, magnetic angle ψ=51.78°, f_{RF}=56MHz (in normalized units: frequency ω'=2πf/$ω_{pi}$=0.168, ω'$_{ci}$=0.1, RF peak-to-peak voltage of V_{pp}/T_e=15). Top: (a) plasma potential, (b) electron density, (c) ion density, as a function of space and time, over one RF period ωt, and 200 Debye lengths along the direction perpendicular to the surface. Bottom: snapshots of the same profiles at selected phases of one RF cycle. Physics model described in: [1] [3]

W First-Ionization Spatial Distribution

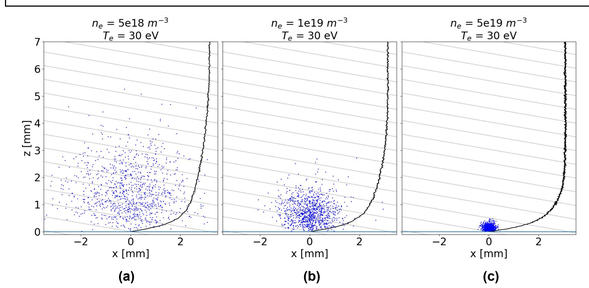

(a) (b) (c)

Figure 5. Spatial distribution of first ionization events (blue dots) with respect to the sheath/presheath potential structure (black like) on a 2D plane (x,z) perpendicular to the divertor surface. Direction of the magnetic lines marked in gray (note that x and z scales are different). First-ionization is intended as the transition from neutral tungesnt (W-I) to tungsten ionized one time Z=+1 (W-II). Electric potential calculated using the hPIC2 code Plasma temperature of T_e=30eV, and density (a) n_e=5x10^{18}m^{-3}, (b) n_e=10^{19}m^{-3}, (c) n_e=5x10^{19}m^{-3}

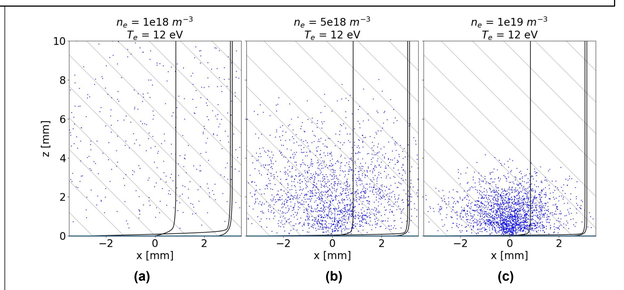

(a) (b) (c)

Figure 8. RF Sheath Spatial distribution of first ionization events (blue dots) with respect to the RF sheath/presheath potential structure (black like) on a 2D plane (x,z) perpendicular to the limiter surface. Direction of the magnetic lines marked in gray (note that x and z scales are different). Electric potential was calculated by numerical modelling of the RF sheath [1] for a plasma temperature of T_e=12eV, and density (a) n_e=1x10^{18}m^{-3}, (b) n_e=5x10^{18}m^{-3}, (c) n_e=10^{19}m^{-3}.

W Prompt Redeposition

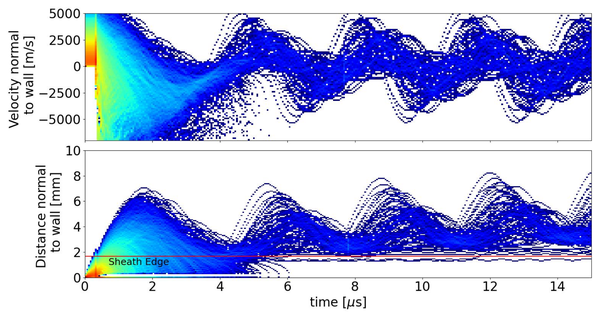

Figure 6. Distance and velocity evolution of sputtered tungsten (W energy sampled from a Thompson distribution) normal to the wall as a function of time in the presence of divertor thermal sheath. Sheath model described in Fig. [4].

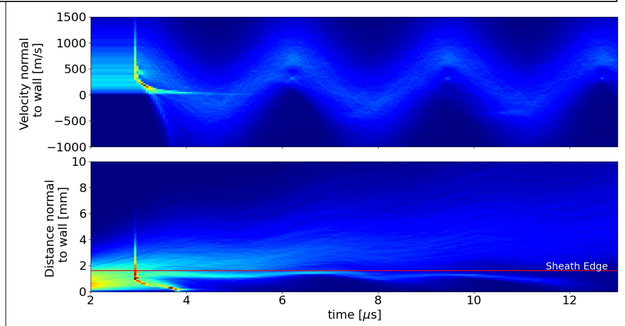

Figure 9. Distance and velocity evolution of sputtered tungsten (W energy sampled from a Thompson distribution) normal to the wall as a function of time in the presence of limiter RF sheath. Sheath model described in Fig. [7].

Next Steps: Understanding impact of W transport in the SOL

- Next step is analyzing the W fluxes leaking from the sheaths of the divertor and RF antenna into the SOL in realistic 3D geometries
- W impurities escaping the sheath region are transported within the SOL on transport time scales, O(10^{-3}s); collisional thermalization of W impurities in the SOL occur on the same time scales, and must be taken into account.
- Tungsten particles, released by the wall at temperatures of T_{wall}~10^{-2}-10^{-1}eV, gain energy via collisions and thermalize into the SOL plasma; see for example our Monte Carlo simulation below (model from [6]), showing the collisional thermalization of W impurities in a 10 eV plasma at 10^{19} m^{-3}.
- The W impurity fluxes reaching the separatrix contribute to core contamination, routinely observed in the experiments via Soft X-Ray.

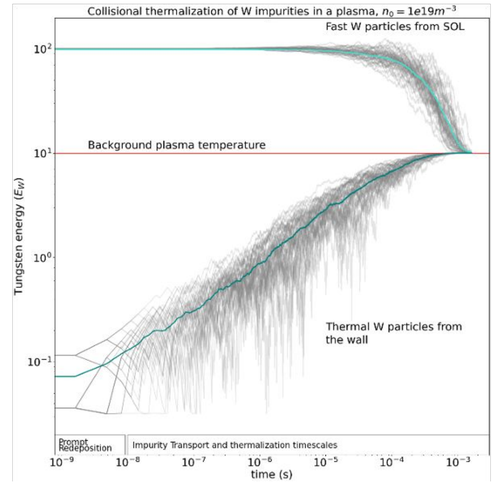

Figure 10. Collisional thermalization of W impurities with a background plasma at 10 eV and 10^{19} m^{-3}. Prompt sheath redeposition discussed in the previous section occurs on very fast time scales, O(10^{-9}-10^{-7} s); transport and thermalization O(10^{-3} s).

Conclusions

- The erosion-redeposition behavior of tungsten in the divertor and limiter regions is affected due to different physics such as sputtered tungsten energy distribution, ionization of the tungsten impurity, effect of sheath dynamics on the impurity.
- RF limiter conditions density is of an order lower than divertor condition which facilitates the tungsten to be ionized much farther away from sheath influence and thus allowing ~60% of the tungsten emitted to possibly enter the SOL.
- Divertor condition ion flux allows for more tungsten to be sputtered compared to limiter region, due to its higher temperature and density. But ionization happens inside the thermal sheath region and gets redeposited promptly allowing only ~0.1% to be able to reach SOL.

References

1) M. Elias, D. Curreli, J. Myra, T. Jenkins, J. Wright, *Numerical Model of the Radio-Frequency Magnetic Presheath Including Wall Impurities*, Physics of Plasmas, Vol. 26, 092508 (2019) https://doi.org/10.1063/1.5109256
2) C. C. Klepper, E. A. Unterberg, Y. Marandet, D. Curreli, A. Grosjean, J. H. Harris, C. A. Johnson, A. Gallo, M. Goniche, Ch. Guillemaut, J. P. Gunn, M. Raghunathan, E. Tsitrone, G. Ciraolo, L. Colas, D. Donovan, A. Ekedahl, D. Easley, G. Urbanczyk, and the WEST Team, Characterizing W sources in the all-W wall, all-RF WEST tokamak environment, Plasma Physics and Controlled Fusion, 64, 104008 (2022) https://doi.org/10.1088/1361-6587/ac8acc
3) J. Myra, "*A tutorial on radio frequency sheath physics for magnetically confined fusion devices*", J. Plasma Phys., vol. 87, 905870504 (2021). https://doi.org/10.1017/S0022377821000878
4) Hillaret et al. Nucl. Fusion 61 (2021) 096030; DOI 10.1088/1741-4326/ac1759
5) S. Di Genova et al 2021 Nucl. Fusion 61 106019; DOI 10.1088/1741-4326/ac2026
6) T.R. Younkin, D.L. Green, A.B. Simpson, B.D. Wirth, *GITR: An accelerated global scale particle tracking code for wall material erosion and redistribution in fusion relevant plasma–material interactions*, Computer Physics Communications, 264 (2021) 107885; https://doi.org/10.1016/j.cpc.2021.107885

U.S. DEPARTMENT OF ENERGY
This material is based upon work supported by the U.S. Department of Energy, Office of Fusion Energy Sciences under Award No. DE-SC0020388.